

Over-hyperthermia using magnetic Fe nanoparticles

Evangelos Hristoforou^{1,*}, Athina Samara², Angelo Ferraro^{3,1}, Athanasios G. Mamalis⁴, Xiaoshan Zhu⁵¹ Laboratory of Physical Metallurgy, National Technical University of Athens, Zografou Campus, Athens 15780, Greece² Current address: Department of Physiology, University of Oslo, Norway³ Lab. of Functional program. materials of quantum electronics for biomedicine. Kazan Federal University, Kazan, 420008, Russian Federation⁴ Project Center for Nanotechnology and Advanced Engineering, NCSR "Demokritos", Athens, Greece⁵ University of Nevada, Reno, Nevada, USA*corresponding author e-mail address: eh@metal.ntua.gr

ABSTRACT

In this work we present a proof-of-concept method for high-temperature hyperthermia and the resultant effect in human dental pulp stem cells. The use of iron super-paramagnetic nanoparticles (ISPAN) instead of super-paramagnetic iron oxide nanoparticles (SPION), in the proper frequency regime, generates temperature elevation much larger than in iron oxide nanoparticles in much shorter time windows, in the order of μs . These outcomes are due to the higher permeability and conductance of ISPAN and result in the so-called over-hyperthermia effect. Provided that ISPAN have been introduced into cells, the large increase of temperature in small volumes and time windows, results in a thermal explosion in the vicinity of the ISPAN, thus causing cell death. This basic principle can be used as a new methodology in targeted drug delivery and hyperthermia. Moreover, the higher magnetic moment of ISPAN could be used for more precise monitoring of their spatial distribution in tissues.

Keywords: iron-nanoparticles, magnetism, hyperthermia, cell-death, Eddy current.

1. INTRODUCTION

The classic hyperthermia is based on magnetic cyclic rotation of the magnetic substance [1], most commonly being Fe_2O_3 or Fe_3O_4 nanoparticles [2], named SPIONs (super-paramagnetic iron oxide nanoparticles), obtained by external alternating magnetic field [3]. Such magnetic rotations cause increase in temperature due to magnetic losses or wear [4]. The obtained and reported increase of temperature is in the order of several Kelvin degrees [5], while control of temperature increase was treated in several ways, one of them being the Curie point of the magnetic substance subjected to external magnetic field [6]. The frequency of the external magnetic field was reported to be from several kHz up to the MHz range [7].

The motivation behind this work was the implementation of the eddy current effects in heating. This way, the proper excitation frequency could cause eddy currents to the first atomic layers of the nanoparticles, permitting large temperature gradient and therefore, sharper temperature profiles with respect to time and space. To that end, our aim was development and heating of iron (Fe) super-paramagnetic nanoparticles (ISPAN) covered with a bi-layer of gold and Poly-Ethylene-Glycol (PEG), aiming at small penetration depths with consequent results on the heat profile of the nanoparticles.

2. EXPERIMENTAL SECTION

The penetration depth δ of eddy currents due to the application of external magnetic field is given by:

$$\delta = \sqrt{\frac{2}{\sigma \omega \mu}} = \sqrt{\frac{\rho}{\pi f \mu}} \quad (1)$$

With $\omega=2\pi f$ referring to the excitation frequency of the external magnetic field and σ , ρ and μ representing specific conductance, specific resistivity and magnetic permeability of the nanoparticle at the mentioned excitation frequency f .

Normally, in nano-size dimensions, the penetration depth is larger than the radius of the magnetic oxide nanoparticles, since permeability and conductance are relatively small. On the contrary, implementation of Fe nanoparticles in nano-size dimensions may allow for high levels of σ and μ , respectively.

Developing and testing Fe nanoparticles can result in $\rho = \frac{1}{\sigma} = 10 \mu \Omega \text{ cm} - 1000 \mu \Omega \text{ cm} = 10^{-7} - 10^{-5} \Omega \text{ m}$, while relative magnetic permeability can reach levels of 10^6 in case of mono-dispersed nanoparticles. In room temperature, ISPAN exhibit

crystalline anisotropy energy kV, where k and V are their anisotropy constant and volume respectively, lower than their thermal activation $k_B T$, where k_B and T are the Boltzmann coefficient and the ambient temperature in K. Therefore, the ordered magnetic moments are randomly flipping in the anisotropy easy axes. In the case of ISPAN, they randomly flip into the 6 directions of the bcc (1,0,0) group of anisotropy directions. They exhibit un-hysteretic magnetic response, with zero remanence and coercivity. When they are subjected to external magnetic field, this flipping freedom is reduced, favouring the magnetization direction. Thus, following the Herzer's law [8], permeability becomes pretty large.

This way, the smallest possible penetration depth δ exhibits values in the order of:

$$\delta = \sqrt{\frac{\rho}{\pi f \mu}} = \sqrt{\frac{10^{-7} \Omega \text{ m}}{\pi f 10^6 \mu_0}} = \sqrt{\frac{10^{-7} \Omega \text{ m}}{\pi f 10^6 2 \pi 10^{-7} \text{ Hm}^{-1}}} = \sqrt{\frac{10^{-7} \Omega \text{ m}}{2 \pi^2 f 10^6 10^{-7} \text{ Hm}^{-1}}} \cong \sqrt{\frac{10^{-7}}{2f}} \text{ m} \quad (2)$$

With f in Hz. Provided that $f \cong 500$ kHz, then:

$$\delta \cong \sqrt{\frac{10^{-7}}{10^6}} \text{ m} = \sqrt{10} \sqrt{10^{-14}} \text{ m} \cong 300 \text{ nm} \quad (3)$$

In such frequency regime, the penetration depth is much larger than the radius of the nanoparticle, thus not permitting eddy current and induction heating effects. But, if the excitation frequency is in the order of 5 GHz, much lower than the ferromagnetic resonance frequency of Fe, the penetration depth equals:

$$\delta = \sqrt{\frac{\rho}{\pi f \mu}} = \sqrt{\frac{10^{-7} \Omega \text{ m}}{\pi f 10^6 \mu_0}} = \sqrt{\frac{10^{-7} \Omega \text{ m}}{\pi f 10^6 2 \pi 10^{-7} \text{ H m}^{-1}}} = \sqrt{\frac{10^{-7} \Omega \text{ m}}{2 \pi^2 f 10^6 10^{-7} \text{ H m}^{-1}}} \cong \sqrt{\frac{10^{-7}}{2f}} \text{ m} \quad (4)$$

This way, in frequencies of 5 GHz and nanoparticles in the order of 10nm, all the applied magnetic field expected losses are transformed to eddy current heating. Thus, the temperature increase can be in the order of 10^3K within 1ms. Therefore, provided that the excitation field is an alternating magnetic field of 0.1ns duration, the temperature increase should exhibit sharp temperature changes in time windows of nanoseconds (ns).

To obtain the same effect in lower frequency (such as 500kHz), the implementation of particles with size dimensions in the order of 1mm is required, as proved above. But, in such dimensions, the particle is not super-paramagnetic, exhibiting hysteresis and significantly lower relative permeability, close to 10-30 (dimensionless). This way, there is no eddy current heating effect in 500kHz, because the penetration depth is very large with respect to the particle diameter.

3. RESULTS SECTION

We used standard culture conditions for 48hrs after passaging, and changed to culture medium containing ISPAN. A representative brightfield and fluorescent image of ISPAN-loaded cells is shown in Figure 2.

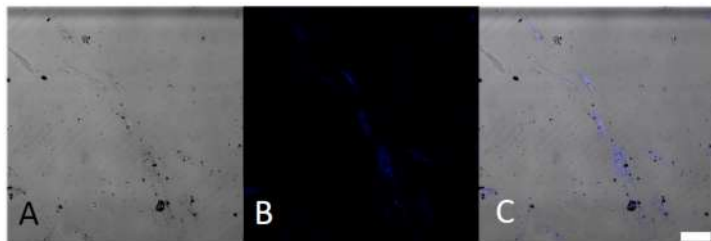


Figure 2. Representative brightfield and fluorescent images of ISPAN-loaded cells. (A) bright-field image showing that nanoparticles have entered the cells; (B) fluorescent micrograph of the same region showing that ISPAN autofluoresce after excitation at 360 nm. (C: A and B merged). Scale bar 10 μm .

PEG-covered ISPAN did not induce cytotoxicity on cultured cells. In fact, cells exposed to ISPAN were healthy for all the testing period. However, we cannot exclude that toxic effects may arise when exposing time is prolong or ISPAN concentration increased. Figure 3 depicts representative fluorescent confocal images showing how ISPAN are distributed on culture cells. Figure 3A is representative of low- and 3B is representative of high- confluency cell culture; a great percentage of ISPAN that

We have developed ISPAN covered with an inner layer of gold to prevent oxidation and an external layer of PEG to increase bioavailability as well as reduce toxicity, using the described chemical vapor deposition (CVD) technology [9]. Accordingly, we used cyclodextrin precursors to capture Fe particles [10], released within the CVD chamber, providing controlled size nanoparticles (Figure 1). They were then covered by a thin PEG layer, and complete coverage was monitored by FTIR analysis [11].

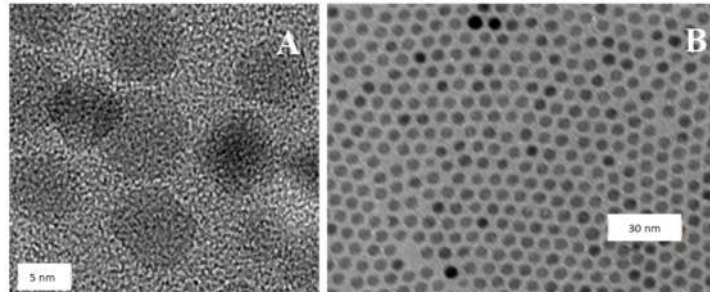


Figure 1. ISPAN developed by chemical vapor deposition, demonstrating a good level of mono-dispersion and size uniformity. Transmission electron microscopy (TEM) images A and B depict the described ISPAN at different magnifications; scale bars are 5nm and 30nm on A and B, respectively.

We used human dental pulp stem cells as biological testing platform of described ISPAN. The cells were cultured in Dulbecco's Modified Eagle Medium (DMEM) supplemented with 10% FBS, incubated at 37°C in a 5% CO_2 ; fluorescent microscope was used to visualize cytoskeleton and nucleus, which were stained post-fixation with 4% paraformaldehyde, with rhodamine phalloidin and DAPI, respectively.

entered cells were concentrated around the nucleus (Figure 3). The intracellular mechanism by which ISPAN were actively transported in the cytosol was not further investigated as it was out of the scope of this work. Indeed, we used human stem cells for the experimental approach as a low cytotoxicity proof of principle.

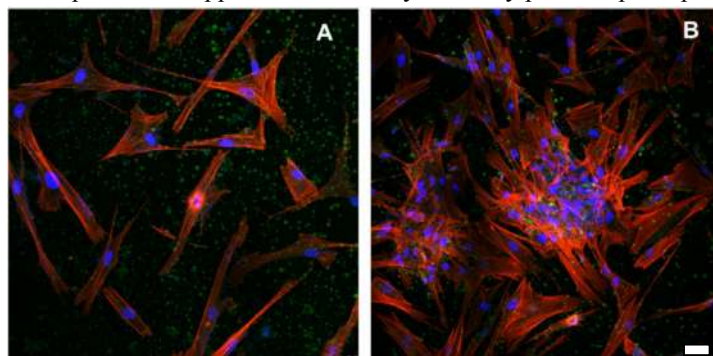


Figure 3. Representative (A) low- and (B) high-confluency stem cell cultures stained with rhodamine phalloidin (for actin cytoskeleton in red) and DAPI (staining nuclei in blue); nanoparticle autofluorescence is depicted in green. Scale bar 20 μm

Nanoparticle heating was performed using a classic valve-operated induction furnace illustrated in Figure 4. The output frequency was industrially set to 500kHz, offering a 10kW output power at this frequency.



Figure 4. The induction valve-based heating device.

Heating up nanoparticles in this frequency did not result in cell damage, as depicted in Figures 5A and 5B. Changing the oscillating conditions of the valve amplifier by changing capacitors and inductors, resulted in higher output frequency at 500MHz with a decrease in power output to <math><1\text{kW}</math> (800-900W), due to the rise time characteristics of the power valve. Heating up nanoparticles in this frequency and power resulted in small holes in the cells as illustrated in Figures 6A and 6B. Thus, even though no direct temperature measurements of ISPAN were performed, when power was reduced one order of magnitude and frequency bandwidth was not high enough, the presence of such small holes within the cells suggested the eddy current heating effect.

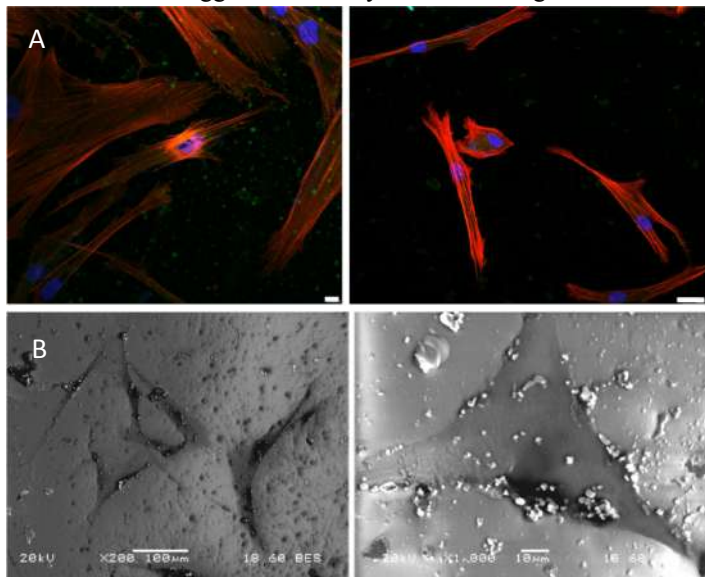


Figure 5. (A) Operation of the induction heating system in relatively low frequencies in the order of 500 kHz did not affect the shape or cytoskeletal integrity of the cultured cells. Scale bars 10 μm left; 20 μm right. (B) Representative SEM images showing relative cell culture nanoparticle dispersion after heating and fixation. Scale bars on the images.

Further modification of the oscillating conditions of the valve amplifier, resulted in 5GHz oscillation but with power decrease down to $\sim 10\text{W}$. Exposing magnetic nanoparticles to such low power resulted in large explosions inside the cells: the small holes of figures 6A and 6B gave way to much larger holes within the cell around and nearing the cell nucleus (Figure 7).

These explosions apparently had detrimental effects on large part of the cytoskeletal architecture as visualized by the rhodamine stain, which revealed discontinuity of fibers and less crisp staining compared to the control-intact cells; this suggests large scale heat increase in very short time, thus possibly concurring with explosions of the cell nucleus. Using scanning

electron microscopy to assess cell damage, we took a closer view of the cells as seen in figure 8.

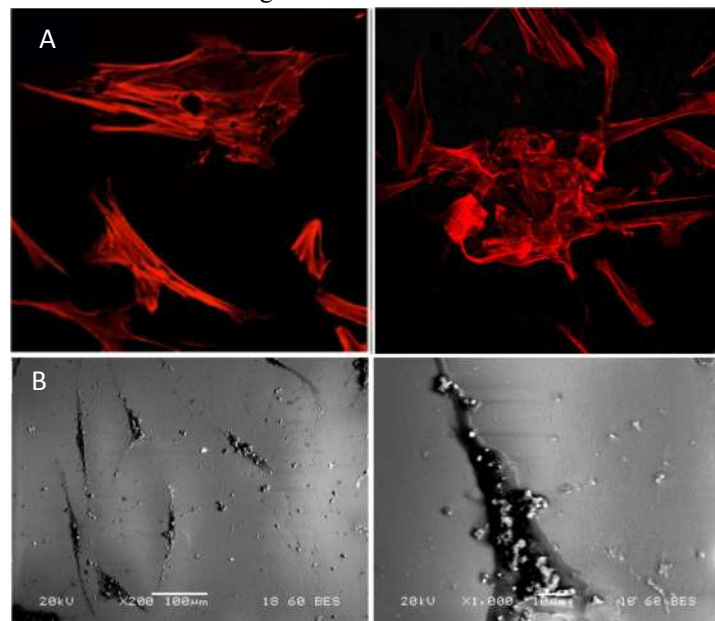


Figure 6. (A) Induced micro-explosions in the cultured cells. (B) Representative SEM images showing relative nanoparticle dispersion cell culture after, heating and fixation.

Furthermore, exposing stem cells without nanoparticles to the same conditions resulted in no cell damage (Figure 9). We believe that our experimental approach has concluded with proof of principle results: the ISPAN loaded cells that had up-taken PEG covered Fe nanoparticles resulted being severely damaged at 5GHz even under alternating field of 10W output power, by means of explosions that affected their nucleus. Meanwhile cells that were not loaded with nanoparticles, when exposed to the same conditions suffered no such damage, as seen in Figure 9. Exposing nanoparticles to 5MHz and power of $\sim 1\text{kW}$ resulted in small holes within the cells, while exposing them to 500kHz resulted in no significant damage under the same culture conditions.

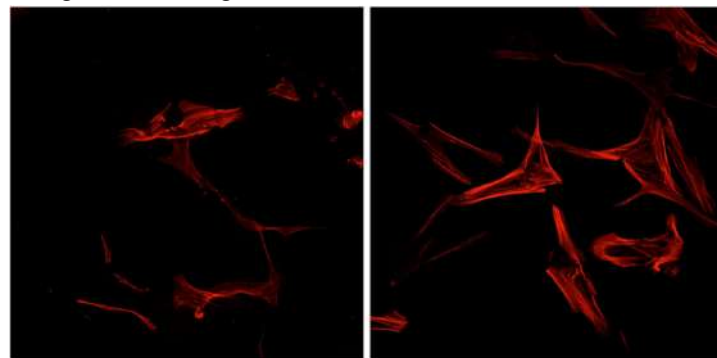


Figure 7. Increasing the excitation frequency to 5 GHz despite the dramatic decrease of power ($<10\text{ W}$ instead of 10 kW for 5 GHz and 500 kHz respectively) resulted in detrimental effects to the cell cytoskeleton; the effect seemed to focus on the cell nucleus.

The main principle of our over-heating methodology is explained by the fact that ISPAN exposed to 10kW magnetic field of 500kHz exhibit small scale temperature increase in large time frames, while nanoparticles exposed to 10W magnetic field of 5GHz exhibit large scale temperature increase in much smaller time frames. These results are in agreement with the supporting theory of eddy current heating due to the small penetration depth and can be further implemented for the development of a new

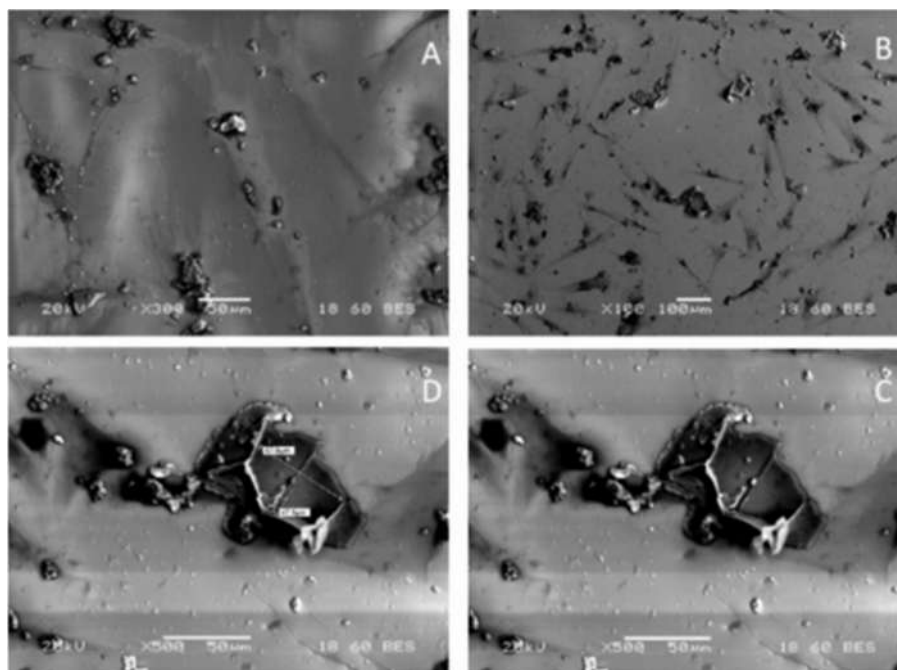


Figure 8. SEM micrographs of human dental pulp stem cells after over-hyperthermia. Increasing the excitation frequency to 5 GHz despite the dramatic decrease of power (10 W instead of 10 kW and 1 kW for 500 kHz and 500 MHz respectively) resulted in detrimental effects; the effect seemed to focus on the cell nucleus. Image A depicts cells where no iron was detected, while iron was present in the cells on image B. Moreover, in some cells, such as in the area encaged in the white rectangle, it was possible to detect membrane folds and craters (magnification shown as image C, and cell crater dimensions shown in D).

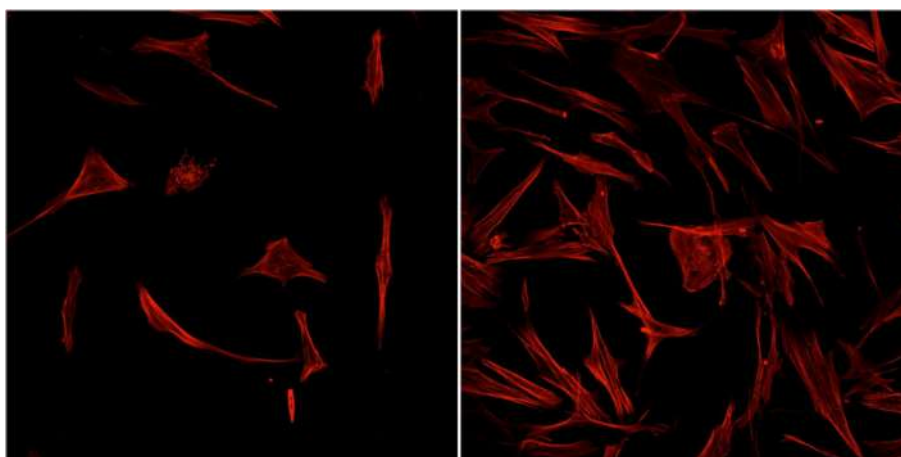


Figure 9. Exposing stem cells without ISPAN in 5 GHz induction field resulted in no cell damage.

4. CONCLUSIONS

The use of gold coated ISPAN instead of SPIONs permits better resolution and monitoring of nanoparticles in the body, when classic resonance techniques are utilized [12]. Therefore, over-hyperthermia resulting in ISPAN explosion coupled with

better monitoring may be explored as a new path for precise cellular ablation, targeted drug delivery and corresponding spatial monitoring.

5. REFERENCES

- [1] Pankhurst Q. A., Connolly J., Jones S. K., Dobson J., Applications of magnetic nanoparticles in biomedicine (Review), *Journal of Physics D: Applied Physics*, 36, 13, R167-R181, **2003**.
- [2] Gupta A. K., Gupta M., Synthesis and surface engineering of iron oxide nanoparticles for biomedical applications, *Biomaterials* 26, 18, 3995-4021, **2005**.
- [3] Rosensweig R. E., Heating magnetic fluid with alternating magnetic field, *Journal of Magnetism and Magnetic Materials*, 252, 1-3 SPEC, ISS, 370-374, **2002**.
- [4] Stefanou G., Sakellari D., Simeonidis K., Kalabaliki T., Angelakeris M., Dendrinou-Samara C., Kalogirou O., Tunable AC magnetic

- hyperthermia efficiency of Ni ferrite nanoparticles *IEEE Transactions on Magnetics*, 50, 12, 1-7, **2014**.
- [5] Bonder M. J., Gallo D., Srinivasan B., Hadjipanayis G. C., Size dependent in-vitro heating with polyethylene glycol coated magnetic nanoparticles, *IEEE Transactions on Magnetics*, 43, 6, 2457-2458, **2007**.
- [6] Astefanoaei I., Dumitru H., Chiriac A., Stancu, Controlling temperature in magnetic hyperthermia with low Curie temperature particles, *Journal of Applied Physics*, 115, 17, 17B531, **2014**.
- [7] Converse M., Bond E. J., Van Veen B. D., Hagness S. C., A computational study of ultra-wideband versus narrowband microwave hyperthermia for breast cancer treatment, *IEEE Transactions on Microwave Theory and Techniques*, 54, 5, 2169-2180, **2006**.

[8] Herzer G., Grain Size Dependence of Coercivity and Permeability in Nanocrystalline Ferromagnets, *IEEE Transactions on Magnetics*, 26, 5, 1397-1402, **1990**.

[9] Papadopoulos N., Karayianni C. S., Tsakiridis P., Sarantopoulou E., Hristoforou E., Effects of MOCVD thin cobalt films' structure and surface characteristics on their magnetic behavior, *Chemical Vapor Deposition*, 17, 7-9, 211-220, **2011**.

[10] Papadopoulos N., Karayianni C. S., Tsakiridis P., Perraki M., Hristoforou E., Cyclodextrin inclusion complexes as novel MOCVD

precursors for potential cobalt oxide deposition, *Applied Organometallic Chemistry*, 24, 2, 112-121, **2010**.

[11] Antipas G. S. E., Statharas E., Tserotas P., Papadopoulos N., Hristoforou E., Experimental and first principles' characterization of functionalized magnetic nanoparticles, *ChemPhysChem*, 14, 9, 1934-1942, **2013**.

[12] Amendola V., Scaramuzza S., Litti L., Meneghetti M., Zuccolotto G., Rosato A., Nicolato E., Marzola P., Fracasso G., Anselmi C., Pinto M., Colombatti M., Magneto-Plasmonic Au-Fe Alloy Nanoparticles Designed for Multimodal SERS-MRI-CT Imaging, *Small*, 10, 12, 2476-2486, **2014**.

© 2016 by the authors. This article is an open access article distributed under the terms and conditions of the Creative Commons Attribution license (<http://creativecommons.org/licenses/by/4.0/>).